Studies of charmed strange baryons in the ΛD final state at Belle

Y. Kato *et al.* (Belle Collaboration)

Phys. Rev. D **94**, 032002 — Published 8 August 2016

DOI: 10.1103/PhysRevD.94.032002

Studies of charmed strange baryons in the ΛD final state at Belle

Y. Kato,[45] T. Iijima,[45,44] I. Adachi,[15,11] H. Aihara,[68] D. M. Asner,[53] V. Aulchenko,[3,52] R. Ayad,[61] I. Badhrees,[61,29] A. M. Bakich,[60] E. Barberio,[40] P. Behera,[20] V. Bhardwaj,[17] B. Bhuyan,[19] J. Biswal,[26] A. Bobrov,[3,52] A. Bondar,[3,52] G. Bonvicini,[73] A. Bozek,[49] M. Bračko,[38,26] T. E. Browder,[14] D. Červenkov,[4] V. Chekelian,[39] B. G. Cheon,[13] K. Chilikin,[35,42] R. Chistov,[35,42] K. Cho,[30] V. Chobanova,[39] S.-K. Choi,[12] Y. Choi,[59] D. Cinabro,[73] J. Dalseno,[39,63] M. Danilov,[42,35] N. Dash,[18] S. Di Carlo,[73] Z. Doležal,[4] Z. Drásal,[4] D. Dutta,[62] S. Eidelman,[3,52] D. Epifanov,[68] H. Farhat,[73] J. E. Fast,[53] T. Ferber,[7] B. G. Fulsom,[53] V. Gaur,[62] N. Gabyshev,[3,52] A. Garmash,[3,52] R. Gillard,[73] R. Glattauer,[23] P. Goldenzweig,[28] O. Grzymkowska,[49] J. Haba,[15,11] K. Hayasaka,[51] H. Hayashii,[46] S. Hirose,[44] W.-S. Hou,[48] G. Inguglia,[7] A. Ishikawa,[66] R. Itoh,[15,11] Y. Iwasaki,[15] I. Jaegle,[14] K. K. Joo,[5] T. Julius,[40] E. Kato,[66] C. Kiesling,[39] D. Y. Kim,[58] J. B. Kim,[31] K. T. Kim,[31] S. H. Kim,[13] Y. J. Kim,[30] K. Kinoshita,[6] P. Kodyš,[4] S. Korpar,[38,26] D. Kotchetkov,[14] P. Križan,[36,26] P. Krokovny,[3,52] T. Kuhr,[37] A. Kuzmin,[3,52] Y.-J. Kwon,[75] J. S. Lange,[9] C. H. Li,[40] H. Li,[21] L. Li,[55] Y. Li,[72] L. Li Gioi,[39] J. Libby,[20] D. Liventsev,[72,15] M. Lubej,[26] T. Luo,[54] M. Masuda,[67] T. Matsuda,[41] D. Matvienko,[3,52] K. Miyabayashi,[46] H. Miyata,[51] R. Mizuk,[35,42,43] G. B. Mohanty,[62] S. Mohanty,[62,71] A. Moll,[39,63] H. K. Moon,[31] R. Mussa,[25] M. Nakao,[15,11] T. Nanut,[26] K. J. Nath,[19] Z. Natkaniec,[49] M. Nayak,[73] M. Niiyama,[32] S. Nishida,[15,11] S. Ogawa,[65] S. Okuno,[27] S. L. Olsen,[56] P. Pakhlov,[35,42] G. Pakhlova,[35,43] B. Pal,[6] C.-S. Park,[75] H. Park,[33] R. Pestotnik,[26] M. Petrič,[26] L. E. Piilonen,[72] C. Pulvermacher,[28] J. Rauch,[64] M. Ritter,[37] A. Rostomyan,[7] Y. Sakai,[15,11] S. Sandilya,[6] L. Santelj,[15] T. Sanuki,[66] V. Savinov,[54] T. Schlüter,[37] O. Schneider,[34] G. Schnell,[1,16] C. Schwanda,[23] Y. Seino,[51] D. Semmler,[9] K. Senyo,[74] O. Seon,[44] I. S. Seong,[14] M. E. Sevior,[40] C. P. Shen,[2] T.-A. Shibata,[69] J.-G. Shiu,[48] A. Sokolov,[24] E. Solovieva,[35,43] M. Starič,[26] M. Sumihama,[10] T. Sumiyoshi,[70] M. Takizawa,[57] K. Tanida,[56] F. Tenchini,[40] K. Trabelsi,[15,11] M. Uchida,[69] S. Uehara,[15,11] T. Uglov,[35,43] Y. Unno,[13] S. Uno,[15,11] P. Urquijo,[40] Y. Usov,[3,52] G. Varner,[14] K. E. Varvell,[60] V. Vorobyev,[3,52] C. H. Wang,[47] P. Wang,[22] M. Watanabe,[51] Y. Watanabe,[27] S. Wehle,[7] K. M. Williams,[72] E. Won,[31] J. Yamaoka,[53] Y. Yamashita,[50] S. Yashchenko,[7] H. Ye,[7] J. Yelton,[8] Y. Yook,[75] C. Z. Yuan,[22] Z. P. Zhang,[55] V. Zhilich,[3,52] V. Zhukova,[42] V. Zhulanov,[3,52] and A. Zupanc[36,26]

(The Belle Collaboration)

[1] *University of the Basque Country UPV/EHU, 48080 Bilbao*
[2] *Beihang University, Beijing 100191*
[3] *Budker Institute of Nuclear Physics SB RAS, Novosibirsk 630090*
[4] *Faculty of Mathematics and Physics, Charles University, 121 16 Prague*
[5] *Chonnam National University, Kwangju 660-701*
[6] *University of Cincinnati, Cincinnati, Ohio 45221*
[7] *Deutsches Elektronen–Synchrotron, 22607 Hamburg*
[8] *University of Florida, Gainesville, Florida 32611*
[9] *Justus-Liebig-Universität Gießen, 35392 Gießen*
[10] *Gifu University, Gifu 501-1193*
[11] *SOKENDAI (The Graduate University for Advanced Studies), Hayama 240-0193*
[12] *Gyeongsang National University, Chinju 660-701*
[13] *Hanyang University, Seoul 133-791*
[14] *University of Hawaii, Honolulu, Hawaii 96822*
[15] *High Energy Accelerator Research Organization (KEK), Tsukuba 305-0801*
[16] *IKERBASQUE, Basque Foundation for Science, 48013 Bilbao*
[17] *Indian Institute of Science Education and Research Mohali, SAS Nagar, 140306*
[18] *Indian Institute of Technology Bhubaneswar, Satya Nagar 751007*
[19] *Indian Institute of Technology Guwahati, Assam 781039*
[20] *Indian Institute of Technology Madras, Chennai 600036*
[21] *Indiana University, Bloomington, Indiana 47408*
[22] *Institute of High Energy Physics, Chinese Academy of Sciences, Beijing 100049*
[23] *Institute of High Energy Physics, Vienna 1050*
[24] *Institute for High Energy Physics, Protvino 142281*
[25] *INFN - Sezione di Torino, 10125 Torino*
[26] *J. Stefan Institute, 1000 Ljubljana*
[27] *Kanagawa University, Yokohama 221-8686*
[28] *Institut für Experimentelle Kernphysik, Karlsruher Institut für Technologie, 76131 Karlsruhe*

[29]King Abdulaziz City for Science and Technology, Riyadh 11442
[30]Korea Institute of Science and Technology Information, Daejeon 305-806
[31]Korea University, Seoul 136-713
[32]Kyoto University, Kyoto 606-8502
[33]Kyungpook National University, Daegu 702-701
[34]École Polytechnique Fédérale de Lausanne (EPFL), Lausanne 1015
[35]P.N. Lebedev Physical Institute of the Russian Academy of Sciences, Moscow 119991
[36]Faculty of Mathematics and Physics, University of Ljubljana, 1000 Ljubljana
[37]Ludwig Maximilians University, 80539 Munich
[38]University of Maribor, 2000 Maribor
[39]Max-Planck-Institut für Physik, 80805 München
[40]School of Physics, University of Melbourne, Victoria 3010
[41]University of Miyazaki, Miyazaki 889-2192
[42]Moscow Physical Engineering Institute, Moscow 115409
[43]Moscow Institute of Physics and Technology, Moscow Region 141700
[44]Graduate School of Science, Nagoya University, Nagoya 464-8602
[45]Kobayashi-Maskawa Institute, Nagoya University, Nagoya 464-8602
[46]Nara Women's University, Nara 630-8506
[47]National United University, Miao Li 36003
[48]Department of Physics, National Taiwan University, Taipei 10617
[49]H. Niewodniczanski Institute of Nuclear Physics, Krakow 31-342
[50]Nippon Dental University, Niigata 951-8580
[51]Niigata University, Niigata 950-2181
[52]Novosibirsk State University, Novosibirsk 630090
[53]Pacific Northwest National Laboratory, Richland, Washington 99352
[54]University of Pittsburgh, Pittsburgh, Pennsylvania 15260
[55]University of Science and Technology of China, Hefei 230026
[56]Seoul National University, Seoul 151-742
[57]Showa Pharmaceutical University, Tokyo 194-8543
[58]Soongsil University, Seoul 156-743
[59]Sungkyunkwan University, Suwon 440-746
[60]School of Physics, University of Sydney, New South Wales 2006
[61]Department of Physics, Faculty of Science, University of Tabuk, Tabuk 71451
[62]Tata Institute of Fundamental Research, Mumbai 400005
[63]Excellence Cluster Universe, Technische Universität München, 85748 Garching
[64]Department of Physics, Technische Universität München, 85748 Garching
[65]Toho University, Funabashi 274-8510
[66]Department of Physics, Tohoku University, Sendai 980-8578
[67]Earthquake Research Institute, University of Tokyo, Tokyo 113-0032
[68]Department of Physics, University of Tokyo, Tokyo 113-0033
[69]Tokyo Institute of Technology, Tokyo 152-8550
[70]Tokyo Metropolitan University, Tokyo 192-0397
[71]Utkal University, Bhubaneswar 751004
[72]Virginia Polytechnic Institute and State University, Blacksburg, Virginia 24061
[73]Wayne State University, Detroit, Michigan 48202
[74]Yamagata University, Yamagata 990-8560
[75]Yonsei University, Seoul 120-749

We report the discovery of $\Xi_c(3055)^0$, observed by its decay into the final state ΛD^0, and present the first observation and evidence of the decays of $\Xi_c(3055)^+$ and $\Xi_c(3080)^+$ into ΛD^+. We also perform a combined analysis of the ΛD^+ with the $\Sigma_c^{++}K^-$ and $\Sigma_c^{*++}K^-$ decay modes to measure the ratios of branching fractions, masses and widths with improved accuracy. We measure the ratios of branching fractions $\mathcal{B}(\Xi_c(3055)^+ \to \Lambda D^+)/\mathcal{B}(\Xi_c(3055)^+ \to \Sigma_c^{++}K^-) = 5.09 \pm 1.01 \pm 0.76$, $\mathcal{B}(\Xi_c(3080)^+ \to \Lambda D^+)/\mathcal{B}(\Xi_c(3080)^+ \to \Sigma_c^{++}K^-) = 1.29 \pm 0.30 \pm 0.15$, and $\mathcal{B}(\Xi_c(3080)^+ \to \Sigma_c^{*++}K^-)/\mathcal{B}(\Xi_c(3080)^+ \to \Sigma_c^{++}K^-) = 1.07 \pm 0.27 \pm 0.04$, where the uncertainties are statistical and systematic. The analysis is performed using a 980 fb^{-1} data sample collected with the Belle detector at the KEKB asymmetric-energy e^+e^- collider.

PACS numbers: 13.30.-a, 14.20.-c

I. INTRODUCTION

In recent years, there has been significant progress in the study of the charmed baryon spectrum, mainly from the Belle and BaBar experiments [1–9]. In the charmed strange baryon sector, a number of excited states (Ξ_c^*) have been observed. Belle reported evidence for two ex-

cited states, $\Xi_c(2980)$ and $\Xi_c(3080)$, in the $\Lambda_c^+ K^- \pi^+$ and $\Lambda_c^+ K_S^0 \pi^-$ final states [2]. These states have been confirmed by BaBar [6]. In the same paper, BaBar also claimed evidence for two resonances, the $\Xi_c(3055)^+$ and the $\Xi_c(3123)^+$, observed in the $\Sigma_c^{++} K^-$ and $\Sigma_c^{*++} K^-$ final states. Recently, Belle confirmed the existence of the $\Xi_c(3055)^+$, but no evidence was found for the $\Xi_c(3123)^+$ [9]. As discussed in Refs. [10, 11], the decay pattern of charmed baryons provides an important contribution to our understanding of the nature of the states. To date, all measurements of Ξ_c^* baryons were performed using decays in which the charm quark is contained in the final-state baryon. Measurements of final states in which the charm quark is part of the final state meson provide complementary information.

In this paper, we report studies of Ξ_c^* baryons decaying to the ΛD^+ and ΛD^0 final states using a data sample with an integrated luminosity of 980 fb^{-1} collected with the Belle detector at the KEKB asymmetric-energy e^+e^- collider. We find significant signals for $\Xi_c(3055)^+$ and $\Xi_c(3080)^+$ decays into ΛD^+. In the ΛD^0 final state, we report observation of the $\Xi_c(3055)^0$. These measurements constitute the first observation and evidence for the $\Xi_c(3055)$ and $\Xi_c(3080)$ into the ΛD final states, and the first-ever observation of the $\Xi_c(3055)^0$. We also perform a combined analysis of the ΛD^+ , $\Sigma_c^{++} K^-$, and $\Sigma_c^{*++} K^-$ final states to measure the ratios of branching fractions and to improve the accuracy of the mass and width measurements.

The remaining sections of the paper are organized as follows. In Sections II and III, we describe the data sample and event selections. In Section IV, observations and measurements of Ξ_c^* baryons in the ΛD^+ and ΛD^0 final states are presented. In Section V, the combined analysis with the $\Sigma_c^{++} K^-$ and $\Sigma_c^{*++} K^-$ final states is presented. Finally, the summary and conclusion are given.

II. DATA SAMPLES AND THE BELLE DETECTOR

We use a data sample with a total integrated luminosity of 980 fb^{-1} recorded with the Belle detector at the KEKB asymmetric-beam-energy e^+e^- collider [12]. The Belle detector is a large-solid-angle magnetic spectrometer that consists of a silicon vertex detector (SVD), a 50-layer central drift chamber (CDC), an array of aerogel threshold Cherenkov counters (ACC), a barrel-like arrangement of time-of-flight scintillation counters (TOF), and an electromagnetic calorimeter comprised of CsI(Tl) crystals (ECL) located inside a superconducting solenoid coil that provides a 1.5 T magnetic field. An iron flux-return located outside of the coil is instrumented to detect K_L^0 mesons and to identify muons. The detector is described in detail elsewhere [13]. Two inner detector configurations were used. A 2.0-cm radius beampipe and a 3-layer silicon vertex detector was used for the first sample of 156 fb^{-1}, while a 1.5-cm radius beampipe, a 4-layer silicon detector and a small-cell inner drift chamber were used to record the remaining 824 fb^{-1} [14].

We use a GEANT-based Monte Carlo (MC) simulation [15] to model the detector response and its acceptance to obtain the reconstruction efficiency and the mass resolution for the signal. We re-weight the signal MC sample according to the scaled-momentum $x_p = p^*/p_{\rm max}$ distributions, based on the measurements in real data, to obtain the correct reconstruction efficiency. Here, p^* is the momentum of the Ξ_c^* system in the center-of-mass frame and $p_{\rm max} = \sqrt{s/4 - M^2c^4}/c$, where s is the total center-of-mass energy squared, M is the invariant mass of the Ξ_c^* system, and c is the speed of light. The generated Ξ_c^* decay angular distribution is flat. We also use MC events generated with EVTGEN [16] and JETSET [17] to study the mass distribution in the background process $e^+e^- \to q\bar{q}$ process ($q = u, d, s, c$ and b).

III. EVENT SELECTION

Our analysis is optimized to search for decays of Ξ_c^* baryons into the ΛD^+ and ΛD^0 final states. Throughout this paper, the inclusion of the charge-conjugate decay mode is implied unless otherwise stated. A Λ candidate is reconstructed via its decay into $p\pi^-$. A D^+ candidate is reconstructed via its decay into $K^-\pi^+\pi^+$. A D^0 candidate is reconstructed via its decay into $K^-\pi^+$, $K^-\pi^+\pi^+\pi^-$, and $K^-\pi^+\pi^0$.

The selection of charged hadrons is based on information from the tracking system (SVD and CDC) and hadron identification system (CDC, ACC, and TOF). The charged hadrons that are not associated with the Λ candidate are required to have a point of closest approach to the interaction point that is within 2 cm along the z axis and within 0.2 cm in the transverse (r-ϕ) plane. The z axis is opposite the positron beam direction. For each track, likelihood values $\mathcal{L}_p$, $\mathcal{L}_K$, and $\mathcal{L}_\pi$ are provided by the hadron identification system, based on the ionization losses in the CDC, the number of detected Cherenkov photons in the ACC, and the time-of-flight measured by the TOF. The likelihood ratio is defined as $\mathcal{L}(i:j) = \mathcal{L}_i/(\mathcal{L}_i + \mathcal{L}_j)$. A track is identified as a proton if the likelihood ratios $\mathcal{L}(p:\pi)$ and $\mathcal{L}(p:K)$ are greater than 0.6, as a kaon if the likelihood ratios $\mathcal{L}(K:\pi)$ and $\mathcal{L}(K:p)$ are greater than 0.6, or as a pion if the likelihood ratios $\mathcal{L}(\pi:K)$ and $\mathcal{L}(\pi:p)$ are greater than 0.6. In addition, an electron likelihood is provided based on information from the ECL, ACC, and CDC [18]. A track with an electron likelihood greater than 0.95 is rejected.

The momentum-averaged efficiencies of hadron identification are about 90%, 90%, and 93% for pions, kaons, and protons, respectively. The momentum-averaged probability to misidentify a pion as a kaon is about 9%, to misidentify a kaon as a pion about 10%, and to misidentify a pion or kaon as a proton about 5%. The π^0 candidates are reconstructed from pairs of photons whose invariant mass ($M_{\gamma\gamma}$) satisfies 120 MeV/$c^2 < M_{\gamma\gamma} <$ 150

MeV/c^2, which corresponds to $\pm 2.5\sigma$ (where σ is the one-standard-deviation of the resolution). The energy of each photon in the laboratory frame is required to be greater than 50 MeV and the energy of the π^0 candidate in the laboratory frame is required to be greater than 500 MeV. The D^+ candidates are selected by requiring $|M(K^-\pi^+\pi^+) - m_{D^+}| < 12$ MeV/c^2, where m_{D^+} is the D^+ mass [19]. The D^0 candidates for each decay mode of the D^0 are selected by requiring $|M(K^-\pi^+) - m_{D^0}| < 14$ MeV/c^2, $|M(K^-\pi^+\pi^+\pi^-) - m_{D^0}| < 11$ MeV/c^2, and $|M(K^-\pi^+\pi^0) - m_{D^0}| < 27$ MeV/c^2, where m_{D^0} is the D^0 mass. These mass ranges correspond to $\pm 2.5\sigma$. To improve the momentum resolution, the daughter particles are fitted to a common vertex together with an invariant mass constrained to the D^+ or D^0 mass. The Λ candidates are selected using cuts on four parameters: the angular difference between the Λ flight direction and the direction pointing from IP to the decay vertex in the transverse plane; the distance between each track and the IP in the transverse plane; the distance between the decay vertex and the IP in the transverse plane; and the displacement along z of the closest-approach points of the two tracks to the beam axis. Also, the invariant mass of a Λ candidate is required to be within 3 MeV/c^2 of the Λ mass, which corresponds to $\pm 3\sigma$. Excited charmed baryons are known to be produced with much higher average momenta than the combinatorial background. We thus require that x_p be greater than 0.7 for the ΛD^+ and 0.8 for the ΛD^0 modes. This requirement removes any possible Ξ_c^* contribution coming from B meson decays.

IV. OBSERVATION OF $\Xi_c t^* \to \Lambda D$ DECAYS

Figure 1 shows the ΛD invariant-mass ($M(\Lambda D)$) distributions for data after the application of all the selection criteria; signals near 3055 and 3080 MeV/c^2 are seen. We do not observe any such peaks in the distributions in wrong-sign $\overline{\Lambda} D$ combinations, in data from the D meson mass sideband, nor in MC events that do not include these resonances. We also check for the possible peaking background from $D_S(2460)^+ \to K_S^0 D^+$ where the K_S^0 is misidentified as a Λ. We find this contribution to be negligible because of the proton identification requirement and the difference of the Q-values of K_S^0 and Λ decays. Hereinafter, Ξ_c^* baryons corresponding to these peaks are referred to as $\Xi_c(3055)$ and $\Xi_c(3080)$. In order to evaluate the masses, widths, and statistical significances of the Ξ_c^* states, we apply an unbinned extended maximum likelihood (UML) fit to the mass spectra in the invariant mass range of 3.0$-$3.2 GeV/c^2. Note that we do not see any contribution from $\Xi_c(2980)$ decays in the lower mass region. For the ΛD^0 mode, the fit is performed simultaneously for the three different D^0 decay modes, with their relative yields fixed using the product of their known branching fractions [19] and detection efficiencies. The masses and widths of the Ξ_c^* states are constrained to be the same for all modes. The detection efficiencies for the $\Xi_c(3055)^0$ and $\Xi_c(3080)^0$ are found to exhibit no difference within the statistical precision of the MC sample, which is smaller than 1%. Therefore, we use common efficiency values for these states. The relative yields are fixed to $K^-\pi^+$:$K^-\pi^+\pi^+\pi^-$:$K^-\pi^+\pi^0$= 1.00:1.30:1.15. The probability density functions (PDF) for the Ξ_c^* components are represented by convolutions of Breit-Wigner shapes with Gaussian distributions to take the intrinsic invariant mass resolution, $\sigma_{\rm res}$, into account. Using the signal MC events, we determine $\sigma_{\rm res}$ for the ΛD^+ mode to be 1.1 MeV/c^2 for the $\Xi_c(3055)^+$ and 1.3 MeV/c^2 for the $\Xi_c(3080)^+$. In the ΛD^0 mode, we determine $\sigma_{\rm res}$ to be 1.1 and 2.0 MeV/c^2 for the D^0 decay mode without and with π^0, respectively for the $\Xi_c(3055)^0$ and 1.3 and 2.2 MeV/c^2 for the $\Xi_c(3080)^0$. The masses, widths and yields of the Ξ_c^* states are treated as free parameters. A third-order Chebyshev polynomial is used to model the PDF for the combinatorial background. The statistical significance is evaluated from $-2\ln(\mathcal{L}_0/\mathcal{L})$, where $\mathcal{L}_0$ ($\mathcal{L}$) is the likelihood for the fit without (with) the signal component. When we evaluate $\mathcal{L}_0$ for one of the Ξ_c^* states, the other Ξ_c^* state is included in the fit. The $-2\ln(\mathcal{L}_0/\mathcal{L})$ values are 144.6 for the $\Xi_c(3055)^+$, 30.0 for the $\Xi_c(3080)^+$, 83.1 for the $\Xi_c(3055)^0$, and 6.6 for the $\Xi_c(3080)^0$. By taking into account the change by 3 of the number of degrees of freedom in the UML fit associated with the inclusion of the Ξ_c^* states, the statistical significances are 11.7σ, 4.8σ, 8.6σ, and 1.7σ for the $\Xi_c(3055)^+$, $\Xi_c(3080)^+$, $\Xi_c(3055)^0$, and $\Xi_c(3080)^0$, respectively. The peak for the $\Xi_c(3080)^0$ is not statistically significant.

We estimate the systematic uncertainty of the masses and widths of $\Xi_c(3055)^0$, $\Xi_c(3055)^+$ and $\Xi_c(3080)^+$ in the ΛD^+ decay mode as the changes produced by giving reasonable variations to the fitting technique. The stability of the background shape is checked by changing the fit region and background PDF. The maximum deviation from the nominal fit is taken as the systematic uncertainty. To check the uncertainty due to $\sigma_{\rm res}$, the ratio $r_\sigma = \sigma_D^{\rm MC}/\sigma_D^{\rm data}$ is evaluated, where $\sigma_D^{\rm MC}$ and $\sigma_D^{\rm data}$ are the D^0 mass resolution for MC and data. For the ΛD^0 mode, r_σ is 1.16, 1.16 and 1.08 for the D^0 final state of $K^-\pi^+$, $K^-\pi^+\pi^+\pi^-$ and $K^-\pi^+\pi^0$, respectively. We evaluate the uncertainty by fitting data with $\sigma_{\rm res}$ scaled by 16% for all the decay modes. To check the uncertainty on the mass due to a possible mis-calibration of the momentum and energy measurements, we check the reconstructed D^0 masses for both data and signal MC. In each mode, the peak position is observed to have a distinct but small deviation from the world average. However, these deviations are well reproduced by the MC and, because of the mass-constrained fit, have little effect on the determination of the masses of the Ξ_c^* baryons. In the signal MC, the differences between the input and output masses of the Ξ_c^* baryons is less than 0.1 MeV/c^2 for all D^0 decay modes. We assign a systematic uncertainty of 0.1 MeV/c^2 on the mass measurements. We perform fits that include the interference of the $\Xi_c(3055)$

and $\Xi_c(3080)$ assuming both resonances have spin 1/2 and decay in S-wave, which maximize the interference effect. The systematic uncertainties are summarized in Table I. The fit result for the $\Xi_c(3080)^+$ width is (1.4 ± 1.8) MeV, which is consistent with zero. Therefore, we set a 90% confidence level upper limit on the width. We redo the fit by changing the width; the width for which the likelihood ratio $-2\ln(\mathcal{L}/\mathcal{L}_{0\Gamma})$ is 2.7, where $L_{0\Gamma}$ is the likelihood with the zero width for $\Xi_c(3080)^+$, is assigned as the 90% confidence level upper limit. We obtain the upper limit $\Gamma_{\Xi_c(3080)^+} < 6.3$ MeV. The measurements of the masses and widths are summarized in Table II. Note that the final values for the $\Xi_c(3055)^+$ and $\Xi_c(3080)^+$ masses and widths in this paper are those combined with $\Sigma_c^{++}K^-$ and $\Sigma_c^{*++}K^-$ decay modes. Values in the ΛD mode only are shown to compare with other decay modes. We find that the mass of the $\Xi_c(3055)^+$ and widths of $\Xi_c(3055)^+$ and $\Xi_c(3080)^+$ are consistent with our previous measurements with the $\Sigma_c^{++}K^-$ and $\Sigma_c^{*++}K^-$ decay modes [9]. However, we find a small inconsistency for the mass of the $\Xi_c(3080)^+$, which may indicate the possible underestimation of the systematic uncertainty for the determination of the masses. We determine the combined value for the masses of the $\Xi_c(3055)^+$ and $\Xi_c(3080)^+$ by taking the weighted average. The uncertainty is scaled by $\sqrt{\chi^2/(N-1)}$, where N is the number of different decay modes, which is 2 for $\Xi_c(3055)^+$ and 3 for $\Xi_c(3080)^+$, if the $\chi^2/(N-1)$ is greater than one; this is the recipe used in Ref. [19]. The scale factor for the $\Xi_c(3055)^+$ is 1.0 and that for the $\Xi_c(3080)^+$ is 3.3. The measured mass of the $\Xi_c(3055)^+$ is (3055.9 ± 0.4) MeV/c^2 and that for $\Xi_c(3080)^+$ is (3077.9 ± 0.9) MeV/c^2. The combined values for the widths are determined by simultaneous fit with $\Sigma_c^{++}K^-$ and $\Sigma_c^{*++}K^-$ decay modes as described in the next section.

V. COMBINED ANALYSIS WITH THE $\Sigma_c^{++}K^-$ AND $\Sigma_c^{*++}K^-$ DECAY MODES

We measure the ratio of branching fractions, $\mathcal{B}(\Xi_c^{*+} \to \Lambda D^+)/\mathcal{B}(\Xi_c^{*+} \to \Sigma_c^{++}K^-) \equiv R_{\mathcal{B}(\Lambda D)}$, using the following equations:

$$R_{\mathcal{B}(\Lambda D)} = R_{\mathrm{yield}(\Lambda D)} \times (\mathcal{B}\times\epsilon)_{\Sigma_c K}/(\mathcal{B}\times\epsilon)_{\Lambda D^+} \quad (1)$$

$$(\mathcal{B}\times\epsilon)_{\Lambda D^+} = \mathcal{B}(D^+ \to K^-\pi^+\pi^+) \times\mathcal{B}(\Lambda \to p\pi^-) \times \epsilon(\Lambda D^+) \quad (2)$$

$$(\mathcal{B}\times\epsilon)_{\Sigma_c K} = \mathcal{B}(\Lambda_c^+ \to pK^-\pi^+) \times [\epsilon_{pK^-\pi^+} + R_{pK_S^0} \times\mathcal{B}(K_S^0 \to \pi^+\pi^-) \times \epsilon_{pK_S^0}], \quad (3)$$

where $\epsilon(\Lambda D^+)$ is the reconstruction efficiency for the ΛD^+ mode, ϵ_i is the reconstruction efficiency for the $\Sigma_c^{++}K^-$ mode with the i^{th} sub-decay of the Λ_c^+, $R_{pK_S^0}$ is the ratio of branching fraction $\mathcal{B}(\Lambda_c^+ \to pK_S^0)/\mathcal{B}(\Lambda_c^+ \to pK^-\pi^+)$ and $R_{\mathrm{yield}(\Lambda D)}$ is the ratio of the yields of Ξ_c^* baryons in the ΛD^+ and the $\Sigma_c^{++}K^-$ modes. For $\mathcal{B}(\Lambda_c^+ \to pK^-\pi^+)$, we use the latest Belle measurement [20]. Other branching fraction values are taken from Ref. [19]. We also measure the ratio of branching fractions, $\mathcal{B}(\Xi_c(3080)^+ \to \Sigma_c^{*++}K^-)/\mathcal{B}(\Xi_c(3080)^+ \to \Sigma_c^{++}K^-) \equiv R_{\mathcal{B}\Sigma_c^* K}$ using the equation

$$R_{\mathcal{B}(\Sigma_c^* K)} = R_{\mathrm{yield}(\Sigma_c^* K)} \times (\mathcal{B}\times\epsilon)_{\Sigma_c K}/(\mathcal{B}\times\epsilon)_{\Sigma_c^* K}, \quad (4)$$

where $R_{\mathrm{yield}(\Sigma_c^* K)}$ is the ratio of yields of $\Xi_c(3080)^+$ in the $\Sigma_c^{*++}K^-$ decay mode and $\Sigma_c^{++}K^-$ decay modes. $(\mathcal{B}\times\epsilon)_{\Sigma_c^* K}$ shares the form of Eq. (3) for $(\mathcal{B}\times\epsilon)_{\Sigma_c K}$ after replacing the reconstruction efficiency for $\Sigma_c^{*++}K^-$ with that for $\Sigma_c^{++}K^-$. The data set used for the $\Sigma_c^{++}K^-$ and $\Sigma_c^{*++}K^-$ decay modes is the same as that for the ΛD^+ mode. Event selections are the same as those in Ref. [9]. A Σ_c^{++} or Σ_c^{*++} candidate is reconstructed via its decay into $\Lambda_c^+\pi^+$; the Λ_c^+ candidate here is reconstructed via its decay into $pK^-\pi^+$ and pK_S^0. Note that the requirement $x_p > 0.7$ is the same as that for the ΛD^+ mode and so it is possible to directly compare the three decay modes. To obtain R_{yield} and to measure the width of the $\Xi_c(3055)^+$ and $\Xi_c(3080)^+$ with greater accuracy than is possible using a single decay mode, we perform a simultaneous UML fit with the widths of the Ξ_c^* states constrained to be the same among the three decay modes, as discussed in the previous section. The masses are not constrained because we find inconsistency for the mass of the $\Xi_c(3080)^+$ among the three decay modes. We also fit the mass distribution of the Σ_c^{++} sideband region, defined as $|M(\Lambda_c^+\pi^+) - (m_{\Sigma_c^{++}} \pm 15\ \mathrm{MeV}/c^2)| < 5$ MeV/c^2, where $m_{\Sigma_c^{++}}$ is the Σ_c^{++} mass, to subtract the contribution from non-resonant $\Lambda_c^+K^-\pi^+$ decays in the signal region. We subtract half of the yield found in the sideband regions because the mass range of the sideband region is double the width of the Σ_c^{++} signal region. It is difficult to define the Σ_c^{*++} sideband regions because the maximum mass that is possible for combinations to contribute to the $\Xi_c(3080)^+$ is only slightly higher than the Σ_c^{*++} mass, and a low mass sideband would overlap with the Σ_c^{++} region. Thus, we estimate the contribution under the Σ_c^{*++} by scaling the yield in the Σ_c^{++} sideband regions by 2.9, a factor estimated using signal MC. We assume no interference between $\Sigma_c^{++}K^-$ or $\Sigma_c^{*++}K^-$ with non-resonant $\Lambda_c^+K^-\pi^+$. The PDFs and fit region for the ΛD^+ are the same as those described in Section IV. The fit conditions for the $\Sigma_c^{++}K^-$ and $\Sigma_c^{*++}K^-$ modes are the same as in Ref. [9]. For the fit to the events from the Σ_c^{++} sideband region, we use the $3.0 - 3.2$ GeV/c^2 $\Sigma_c^{++}K^-$ mass range. The Ξ_c^* contributions are represented by a Gaussian-convolved Breit-Wigner with the same mass resolution of the Ξ_c^* states as that used for the Σ_c^{++} signal region. The combinatorial background is represented by a second-order Chebyshev polynomial. Figure 2 shows the results of the simultaneous fit.

The following systematic uncertainties are taken into account for the combined analysis for the measure-

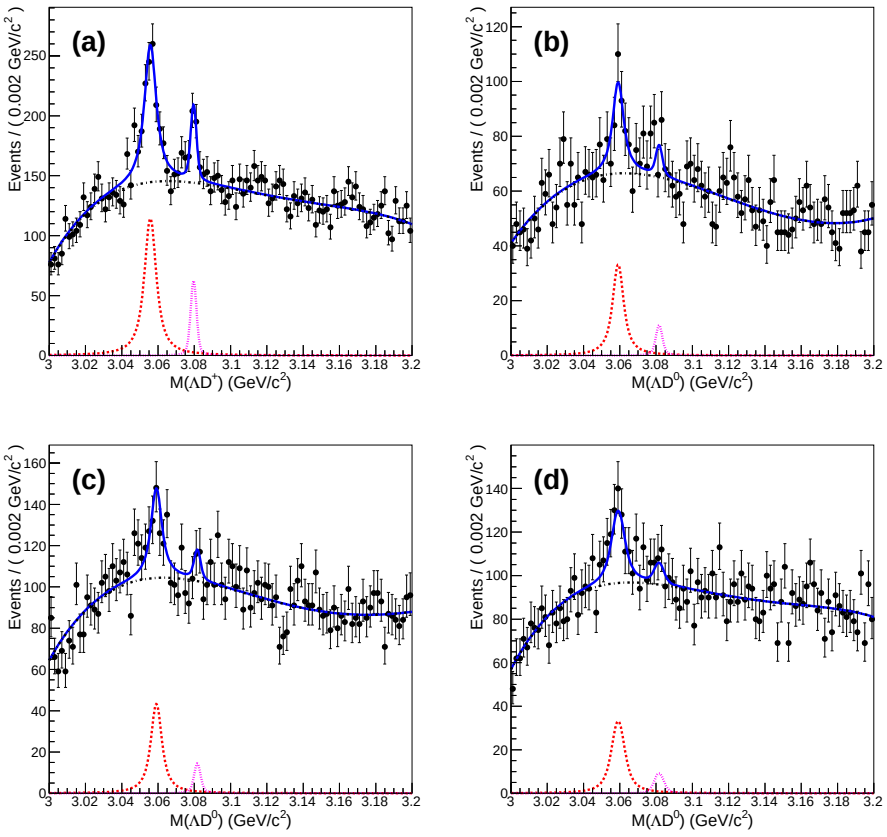

FIG. 1: $M(\Lambda D)$ distributions. Points with statistical error bars are data. Blue solid lines show the fit results. The red dashed, magenta dotted, and black dashed-dotted lines show the $\Xi_c(3055)$ signal, the $\Xi_c(3080)$ signal, and the background components, respectively. (a) $M(\Lambda D^+)$ distribution; $M(\Lambda D^0)$ distributions for the (b) $K^-\pi^+$, (c) $K^-\pi^+\pi^+\pi^-$, and (d) $K^-\pi^+\pi^0$ D^0 decay modes.

TABLE I: Systematic uncertainties for the mass (MeV/c^2) and width (MeV) of the Ξ_c^*.

Source	$M_{\Xi_c(3055)^0}$	$\Gamma_{\Xi_c(3055)^0}$	$M_{\Xi_c(3055)^+}$	$\Gamma_{\Xi_c(3055)^+}$	$M_{\Xi_c(3080)^+}$
Background shape	0.6	1.0	0.1	1.5	0.0
Resolution	0.0	0.2	0.0	0.2	0.0
Mass scale	0.1	0.0	0.1	0.0	0.1
Interference	0.1	0.3	0.1	0.1	0.1
Total	0.6	1.1	0.2	1.5	0.1

ments of the ratios of branching fractions and width. The systematic uncertainty due to the pion- and kaon-identification efficiency is estimated from the ratio of the yields of the $D^{*+} \to D^0\pi^+$, $D^0 \to K^-\pi^+$ with and without the pion- and kaon-identification requirements for data and MC. The difference of the ratio between data and MC is used to correct the efficiency and the statistical error of this correction is treated as the systematic uncertainty. We conservatively assume no correlation in the systematic uncertainty for pion and kaon identification between ΛD^+ and $\Sigma_c^{++}K^-$ decay modes as the momentum ranges for these decay modes are distinct; the systematic uncertainty for $\Sigma_c^{++}K^-$ and $\Sigma_c^{*++}K^-$ cancel. The systematic uncertainty due to the efficiency of proton identification is determined using the ratio of the yields of the $\Lambda \to p\pi^-$ with and without the proton identification requirement. The difference of the ratio between data and MC is used to correct the efficiency and the statistical uncertainty of this correction is regarded as the systematic uncertainty. The systematic uncertainty due to the reconstruction efficiency of the Λ is determined using the yield ratio of $B \to \Lambda\bar{\Lambda}K^+$ with and without the Λ selection cut as a function of momenta of Λ. By taking the weighted average of the momentum, it is estimated to be 3%. The uncertainties of the branching fractions [19, 20] are included as systematic uncertainties. The stability of

TABLE II: Summary of the masses, widths and significances of the Ξ_c^* baryons measured in the ΛD modes. The first error is statistical and the second is systematic. We set a 90% confidence level upper limit for the width of $\Xi_c(3080)^+$.

Resonance	Mass (MeV/c^2)	Width (MeV)	Significance (σ)
$\Xi_c(3055)^0$	$3059.0 \pm 0.5 \pm 0.6$	$6.4 \pm 2.1 \pm 1.1$	8.6
$\Xi_c(3055)^+$	$3055.8 \pm 0.4 \pm 0.2$	$7.0 \pm 1.2 \pm 1.5$	11.7
$\Xi_c(3080)^+$	$3079.6 \pm 0.4 \pm 0.1$	< 6.3	4.8

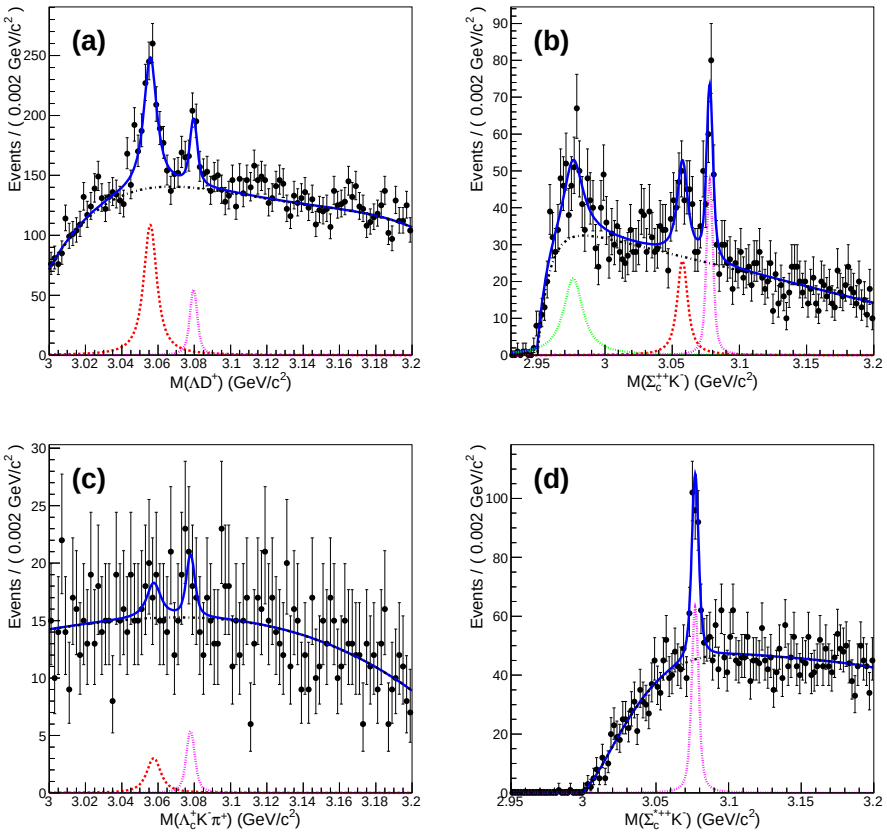

FIG. 2: The simultaneous fit results. Points with error bars are data. The blue solid lines show the fit result. The red dashed, magenta dotted, green dotted, and black dash-dotted lines show the contributions from the $\Xi_c(3055)^+$, $\Xi_c(3080)^+$, $\Xi_c(2980)^+$, and background, respectively. (a) $M(\Lambda D^+)$, (b) $M(\Sigma_c^{++}K^-)$, (c) $M(\Lambda_c^+K^-\pi^+)$ for the Σ_c^{++} sideband region, and (d) $M(\Sigma_c^{*++}K^-)$.

the background shape is checked by changing the fit region and background PDF. The maximum deviation from the nominal fit among the various changes is regarded as the systematic uncertainty. To assess the uncertainty due to $\sigma_{\rm res}$, r_σ is evaluated as $\sigma_D^{MC}/\sigma_D^{data} = 1.15$ for the ΛD^+ mode and $\sigma_{\Lambda_c^+}^{MC}/\sigma_{\Lambda_c^+}^{data} = 1.08$ for the $\Sigma_c^{++}K^-$; we perform a fit with $\sigma_{\rm res}$ scaled by a factor of r_σ and use the difference of the result from the nominal fit as the systematic uncertainty. To check the uncertainty due to a possible mis-calibration of momentum and energy measurements, we evaluate the difference between the reconstructed and nominal D^+ and Λ_c^+ masses for both data and MC. In data, the reconstructed D^+ mass differs from the world average [19] by 0.1 MeV/c^2 whereas, in the MC, the D^+ mass differs by 0.2 MeV/c^2. No deviation is observed for Λ_c^+ for both data and MC. In the signal MC, the difference of the input and output Ξ_c^* masses in the ΛD^+ mode is 0.1 MeV/c^2, which is smaller than the deviation observed in the D^+ mass because of the mass-constrained fit. We conservatively assign the systematic uncertainty of 0.1 MeV/c^2 on the mass measurement. The systematic uncertainty on the ratio of branching fraction due to the possibility that the Ξ_c^* is polarized is evaluated by producing signal MC events with various assumptions on the spin density matrix with spin 3/2 and 5/2. The maximum difference of the reconstruction efficiency from the one obtained for the flat decay angular distribution

is regarded as the systematic uncertainty.

Table III summarizes the systematic uncertainties. Table IV summarizes the measurement of yields and widths of the $\Xi_c(3055)^+$ and $\Xi_c(3080)^+$ and Table V summarizes the values related to the ratio of branching fractions measurements.

VI. SUMMARY AND CONCLUSIONS

We present studies of Ξ_c^* baryons decaying into the ΛD^+ and ΛD^0 final states. We report the first observation of the $\Xi_c(3055)^0$ in the ΛD^0 mode with a significance of 8.6σ. The mass and width of the $\Xi_c(3055)^0$ are measured to be $(3059.0\pm0.5\pm0.6)$ MeV/c^2 and $(6.4\pm2.1\pm1.1)$ MeV, respectively. We report the first observation of the $\Xi_c(3055)^+$ decay and evidence for the $\Xi_c(3080)^+$ in the ΛD^+ final state. The mass and width of the $\Xi_c(3055)^+$ obtained from the ΛD final states only are $(3055.8\pm0.4\pm0.2)$ MeV/c^2 and $(7.0\pm1.2\pm1.5)$ MeV, respectively, and those for $\Xi_c(3080)^+$ are $(3079.6\pm0.4\pm0.1)$ MeV/c^2 and < 6.3 MeV, respectively. The measured values for $\Xi_c(3055)^+$ are more accurate than the world average thanks to the high statistics in this decay mode.

We perform a combined analysis of these particles by comparing their decays into ΛD^+ with those into $\Sigma_c^{++}K^-$ and $\Sigma_c^{*++}K^-$. We measure the ratios of branching fractions $\mathcal{B}(\Xi_c(3055)^+ \to \Lambda D^+)/\mathcal{B}(\Xi_c(3055)^+ \to \Sigma_c^{++}K^-) = 5.09 \pm 1.01 \pm 0.76$, $\mathcal{B}(\Xi_c(3080)^+ \to \Lambda D^+)/\mathcal{B}(\Xi_c(3080)^+ \to \Sigma_c^{++}K^-) = 1.29\pm0.30\pm0.15$, and $\mathcal{B}(\Xi_c(3080)^+ \to \Sigma_c^{*++}K^-)/\mathcal{B}(\Xi_c(3080)^+ \to \Sigma_c^{++}K^-) = 1.07 \pm 0.27 \pm 0.04$. The width of the $\Xi_c(3055)^+$ is $(7.8\pm1.2\pm1.5)$ MeV and that of the $\Xi_c(3080)^+$ is $(3.0\pm0.7\pm0.4)$ MeV. We take the weighted average of the measurements in the different decay modes to find the masses of the $\Xi_c(3055)^+$ and $\Xi_c(3080)^+$ to be (3055.9 ± 0.4) MeV/c^2 and (3077.9 ± 0.9) MeV/c^2, respectively, where the uncertainties are scaled by $\sqrt{\chi^2/(N-1)}$ to account for small inconsistencies in the N individual measurements. The uncertainties on the masses incorporate the statistical and systematic values. The masses and widths of $\Xi_c(3055)^+$ and $\Xi_c(3080)^+$, after combining other decay modes, supersede our previous measurements [9].

Our measurements provide information on the nature of these baryons. For instance, the chiral quark model has been used to identify the $\Xi_c(3055)$ as the D-wave excitation in the N=2 shell, and predicts $\mathcal{B}(\Xi_c(3055) \to \Sigma_c\bar{K})$:$\mathcal{B}(\Xi_c(3055) \to \Lambda D)$ to be 2.3:0.1 or 5.6:0.0, depending on the possible excitation modes [11]. It further identifies the $\Xi_c(3080)$ as an S-wave excitation mode of the Ξ_c in N=2 shell and predicts that its decay into ΛD is forbidden. Both of these predictions are in contradiction with our measurements. Further experimental and theoretical work is needed to understand these baryons.

Acknowledgments

We thank the KEKB group for the excellent operation of the accelerator; the KEK cryogenics group for the efficient operation of the solenoid; and the KEK computer group, the National Institute of Informatics, and the PNNL/EMSL computing group for valuable computing and SINET4 network support. We acknowledge support from the Ministry of Education, Culture, Sports, Science, and Technology (MEXT) of Japan, the Japan Society for the Promotion of Science (JSPS), and the Tau-Lepton Physics Research Center of Nagoya University; the Australian Research Council; Austrian Science Fund under Grant No. P 22742-N16 and P 26794-N20; the National Natural Science Foundation of China under Contracts No. 10575109, No. 10775142, No. 10875115, No. 11175187, No. 11475187 and No. 11575017; the Chinese Academy of Science Center for Excellence in Particle Physics; the Ministry of Education, Youth and Sports of the Czech Republic under Contract No. LG14034; the Carl Zeiss Foundation, the Deutsche Forschungsgemeinschaft, the Excellence Cluster Universe, and the VolkswagenStiftung; the Department of Science and Technology of India; the Istituto Nazionale di Fisica Nucleare of Italy; the WCU program of the Ministry of Education, National Research Foundation (NRF) of Korea Grants No. 2011-0029457, No. 2012-0008143, No. 2012R1A1A2008330, No. 2013R1A1A3007772, No. 2014R1A2A2A01005286, No. 2014R1A2A2A01002734, No. 2015R1A2A2A01003280 , No. 2015H1A2A1033649; the Basic Research Lab program under NRF Grant No. KRF-2011-0020333, Center for Korean J-PARC Users, No. NRF-2013K1A3A7A06056592; the Brain Korea 21-Plus program and Radiation Science Research Institute; the Polish Ministry of Science and Higher Education and the National Science Center; the Ministry of Education and Science of the Russian Federation and the Russian Foundation for Basic Research; the Slovenian Research Agency; Ikerbasque, Basque Foundation for Science and the Euskal Herriko Unibertsitatea (UPV/EHU) under program UFI 11/55 (Spain); the Swiss National Science Foundation; the Ministry of Education and the Ministry of Science and Technology of Taiwan; and the U.S. Department of Energy and the National Science Foundation. This work is supported by a Grant-in-Aid for Scientific Research (S) "Probing New Physics with Tau-Lepton" (No.26220706), Grant-in-Aid for Scientific Research on Innovative Areas "Elucidation of New Hadrons with a Variety of Flavors", Grant-in-Aid from MEXT for Science Research in a Priority Area ("New Development of Flavor Physics") and from JSPS for Creative Scientific Research ("Evolution of Tau-lepton Physics").

TABLE III: Summary of the systematic uncertainties for the width (MeV) and ratio of branching fraction ratios (%) measurements from the combined analysis.

Source	$\Gamma_{\Xi_c(3055)^+}$	$R_{\mathcal{B}(\Lambda D)}$ for $\Xi_c(3055)^+$	$\Gamma_{\Xi_c(3080)^+}$	$R_{\mathcal{B}(\Lambda D)}$ for $\Xi_c(3080)^+$	$R_{\mathcal{B}(\Sigma_c^* K)}$
πKp identification	-	1.4	-	1.4	-
Λ identification	-	3.0	-	3.0	-
Branching fractions	-	5.7	-	5.7	-
Background shape	1.5	13.1	0.4	9.7	1.0
Resolution	0.2	2.1	0.2	1.6	0.5
Mass scale	0.0	0.0	0.0	0.0	0.0
Polarization	-	1.6	-	1.6	3.5
Total	1.5	14.9	0.4	12.0	3.7

TABLE IV: Summary of results from the simultaneous fits to the ΛD^+ and $\Sigma_c^{++} K^-$ modes.

Resonance	Width (MeV)	Yield for ΛD^+	Yield for $\Sigma_c^{++} K^-$	Yield for sideband	Yield for Σ_c^{*++}
$\Xi_c(3055)^+$	$7.8 \pm 1.2 \pm 1.5$	721 ± 90	173 ± 30	21 ± 18	-
$\Xi_c(3080)^+$	$3.0 \pm 0.7 \pm 0.4$	186 ± 40	176 ± 23	20 ± 12	234 ± 30

[1] R. Mizuk *et al.* [Belle Collaboration], Phys. Rev. Lett. **94**, 122002 (2005) [hep-ex/0412069].

[2] R. Chistov *et al.* [Belle Collaboration], Phys. Rev. Lett. **97**, 162001 (2006) [hep-ex/0606051].

[3] B. Aubert *et al.* [BaBar Collaboration], Phys. Rev. Lett. **97**, 232001 (2006) [hep-ex/0608055].

[4] B. Aubert *et al.* [BaBar Collaboration], Phys. Rev. Lett. **98**, 012001 (2007) [hep-ex/0603052].

[5] K. Abe *et al.* [Belle Collaboration], Phys. Rev. Lett. **98**, 262001 (2007) [hep-ex/0608043].

[6] B. Aubert *et al.* [BaBar Collaboration], Phys. Rev. D **77**, 012002 (2008) [arXiv:0710.5763 [hep-ex]].

[7] E. Solovieva *et al.*, Phys. Lett. B **672**, 1 (2009) [arXiv:0808.3677 [hep-ex]].

[8] T. Lesiak *et al.* [Belle Collaboration], Phys. Lett. B **665**, 9 (2008) [arXiv:0802.3968 [hep-ex]].

[9] Y. Kato *et al.* [Belle Collaboration], Phys. Rev. D **89**, 052003 (2014) [arXiv:1312.1026 [hep-ex]].

[10] H.-Y. Cheng and C.-K. Chua, Phys. Rev. D **75**, 014006 (2007) [hep-ph/0610283].

[11] L.-H. Liu, L. -Y. Xiao and X.-H. Zhong, Phys. Rev. D **86**, 034024 (2012) [arXiv:1205.2943 [hep-ph]].

[12] S. Kurokawa and E. Kikutani, Nucl. Instr. and. Meth. A**499**, 1 (2003), and other papers included in this volume; T. Abe *et al.*, Prog. Theor. Exp. Phys. (2013) 03A001 and following articles up to 03A011.

[13] A. Abashian *et al.* [Belle Collaboration], Nucl. Instr. and Meth. A **479**, 117 (2002); also see detector section in J. Brodzicka *et al.*, Prog. Theory. Exp. Phys. (2012) 04D001.

[14] Z. Natkaniec *et al.* (Belle SVD2 Group), Nucl. Instr. and Meth. A **560**, 1 (2006).

[15] R. Brun *et al.*, GEANT3.21, CERN Report DD/EE/84-1 (1984).

[16] D. J. Lange, Nucl. Instr. and. Meth. A **462**, 152 (2001).

[17] T. Sjøstrand, Comput. Phys. Commun. **82**, 74 (1994).

[18] K. Hanagaki, H. Kakuno, H. Ikeda, T. Iijima and T. Tsukamoto, Nucl. Instr. and. Meth. **485**, 490 (2002) [hep-ex/0108044].

[19] K. A. Olive *et al.* [Particle Data Group], Chin. Phys. C **38**, 090001 (2014).

[20] A. Zupanc *et al.* [Belle Collaboration], Phys. Rev. Lett. **113**, 042002 (2014) [arXiv:1312.7826 [hep-ex]].

TABLE V: Summary of the values related to the measurements of the ratio of branching fractions. The branching fraction values are taken from Ref. [19, 20]. For the ratios of branching fractions, the first error is statistical and second is systematic.

Variable	Value
$\mathcal{B}(D^+ \to K^-\pi^+\pi^+)$	0.0913 ± 0.0019
$\mathcal{B}(\Lambda \to p\pi^-)$	0.639 ± 0.005
$\mathcal{B}(\Lambda_c^+ \to pK^-\pi^+)$	0.0684 ± 0.036
$\mathcal{B}(K_S^0 \to \pi^+\pi^-)$	0.6920 ± 0.0005
$\mathcal{B}(\Lambda_c^+ \to pK_S^0)/\mathcal{B}(\Lambda_c^+ \to pK^-\pi^+)$	0.24 ± 0.02
$\epsilon(\Lambda D^+)$	0.1771
$\epsilon_{pK^-\pi^+}\ (\Sigma_c^{++}K^-)$	0.149
$\epsilon_{pK_S^0}\ (\Sigma_c^{++}K^-)$	0.155
$\epsilon_{pK^-\pi^+}\ (\Sigma_c^{*++}K^-)$	0.146
$\epsilon_{pK_S^0}\ (\Sigma_c^{*++}K^-)$	0.153
$(\mathcal{B}\times\epsilon)_{\Lambda D^+}$	0.0103
$(\mathcal{B}\times\epsilon)_{\Sigma_c K}$	0.0119
$(\mathcal{B}\times\epsilon)_{\Sigma_c^* K}$	0.0117
$R_{\mathrm{yield}(\Lambda D)}$ for $\Xi_c(3055)^+$	4.41 ± 0.87
$R_{\mathrm{yield}(\Lambda D)}$ for $\Xi_c(3080)^+$	1.12 ± 0.26
$R_{\mathrm{yield}(\Sigma_c^* K)}$	1.05 ± 0.27
$R_{\mathcal{B}(\Lambda D)}$ for $\Xi_c(3055)^+$	$5.09 \pm 1.01 \pm 0.76$
$R_{\mathcal{B}(\Lambda D)}$ for $\Xi_c(3080)^+$	$1.29 \pm 0.30 \pm 0.15$
$R_{\mathcal{B}(\Sigma_c^* K)}$	$1.07 \pm 0.27 \pm 0.04$